Environmental Earth Sciences (2019) 78:515
https://doi.org/10.1007/s12665-019-8531-6

ORIGINAL ARTICLE

Arsenic redistributive accretion in interdune marshes and its impact on groundwater contamination of coastal plains (southern Brazil)

Ingrid Horák-Terra[1] · Nicolai Mirlean[2] · Alexandre Henrique Ferraz[2]

Received: 30 October 2018 / Accepted: 3 August 2019 / Published online: 9 August 2019
© Springer-Verlag GmbH Germany, part of Springer Nature 2019

Abstract

Excessive concentrations of arsenic in aquifers have been presented for the first time in the southern Brazilian coastal plain. In this region, the shallow aquifers are mainly constituted by a mosaic distribution of marsh sediment lenses formed in the interdune depressions in past times and subsequently covered by eolian sands. The stratigraphic descriptions and analytical determinations in water (pH, conductivity, As) and sediment (organic carbon, As, Fe, Mn) were obtained in samples of an interdune freshwater marsh, an aquifer (a palaeo-freshwater marsh), and a modern eolic dune. Principal component analysis was applied to summarize the process of As immobilization. In sediments of the modern interdune marshes and under suboxic conditions, As is mobilized from the eolic sands and its redistribution occurs along sediment profile. Its maximum concentration (up to 1.7 mg kg^{-1} dw) occurred at the marsh's sediments surface and was strongly coupled to Fe hydroxides. In pore water of marshes, As has been registered up to 79 µg L^{-1}. This enrichment was driven by reductive dissolution of As-bearing Fe hydroxides in sediments, where the reduced environment has allowed their desorption from solids as Fe(II) and As(III) reduction. After the cover of the interdune marshes by eolic sands, turning them into current aquifers, the high As contents have been maintained above the sanitary limit of 10 µg L^{-1} for drinking water in groundwaters. The southern Brazilian coastal plain is probably an area with arsenic contamination problem for groundwater, which deserves more attention when it is used for drinking supply.

Keywords Coastal plain · Marshes · Arsenic · Redistribution · Groundwater · Contamination

Introduction

One of the main sources of drinking water is the groundwater, and the presence of arsenic (As) is worrying taking into account populations at risk of exposure to its excessive levels (Smedley and Kinniburgh 2002). Chronic exposure to As by drinking water may result in adverse health impacts such as arsenicosis, and some cancers besides (Morton and Dunette 1994; Das et al. 1995; Smith et al. 1998). The World Health Organization Guideline (2011) has recommended the threshold value of 10 µg L^{-1} for As in waters for human consumption. In recent years, Asian countries such as Bangladesh, India, China, Pakistan, Taiwan, Vietnam, and Nepal have been focus of numerous researches about As contamination (Nickson et al. 1998; Smedley and Kinniburgh 2002; Nickson et al. 2005; Bhattacharya et al. 2009; Rodríguez-Lado et al. 2013; Lin et al. 2013; Diwakar et al. 2015) showing many contaminated aquifers. Besides, other countries such as USA, Hungary, Chile, Argentina, and Mexico have also

Electronic supplementary material The online version of this article (https://doi.org/10.1007/s12665-019-8531-6) contains supplementary material, which is available to authorized users.

✉ Ingrid Horák-Terra
ingrid.horak@ufvjm.edu.br

Nicolai Mirlean
dgeonmir@furg.br

Alexandre Henrique Ferraz
aleferraz.h@gmail.com

[1] Present Address: Institute of Agricultural Sciences, Federal University of Jequitinhonha and Mucuri Valleys-ICA/UFVJM, Av. Vereador João Narciso, 1380, Unaí, MG 38610000, Brazil

[2] Institute of Oceanography, Federal University of Rio Grande-IO/FURG, Rio Grande, RS 96203900, Brazil

received attention because of it (Smedley and Kinniburgh 2002; Johannesson and Tang 2009; Kumar et al. 2010).

Few areas with As pollution problems were detected in Brazil, and these are mainly related to the mining environments. High concentrations of As in groundwater were found in the "Iron Quadrangle" in Minas Gerais state, one of the most important long-term mineral resource regions of the world (Bundschuh et al. 2012). They are related to ore deposits where As is predominantly contained in sulfidic minerals such as arsenopyrite and pyrite (Borba et al. 2003). Some other regions have also been investigated in Brazil, Ribeira valley (southeastern) and Amazon (northern) among them, where As occurs in Pb–Zn mine wastes and in association with mined manganese ores (de Figueiredo et al. 2007). For the first time in Brazil, high concentrations of As were registered in groundwater up to 600 µg L^{-1} due to natural contamination in the Baixada Fluminense coastal plain (Paraiba do Sul delta in Rio de Janeiro state) (Mirlean et al. 2014).

Two main geochemical conditions are known to be associated with natural As enrichment in groundwater systems (Rodríguez-Lado et al. 2013): (1) aerobic alkaline environments in closed basins in arid and semiarid regions, where high pH leads to alkaline desorption of As from oxide minerals, and (2) aquifers with reducing conditions, where the release of As is related to reductive dissolution of As-bearing iron hydroxides in sediments (Smedley and Kinniburgh 2002; Guo et al. 2011; Rodríguez-Lado et al. 2013). This latter is probably the mechanism of As release to groundwater in the Baixada Fluminense plain (Mirlean et al. 2014).

Values up to 273 mg kg^{-1} from sediments were determined in Keratea-Lavrio, one of the Attica streams, in Greece (Alexakis 2011). According to Alexakis (2011) and Alexakis and Gamvroula (2014), both natural and anthropogenic are sources of As input in this region. By hydrochemical analysis, statistical analysis, and GIS database, Gamvroula et al. (2013) verified that several factors and mechanisms control the distribution of major and trace elements in groundwater and that the knowledge of these is necessary in each type of environment.

Along the margins of the Patos lagoon, a beach ridge complex of relic nature, dating from Quaternary, characterizes the coastal plain of the southern Brazil (Buchmann et al. 2009). Between the ridges, freshwater marshes are formed in the interdune depressions, locally called "*banhados*", and characterized as periodically inundated areas (higher saturation in the months with greater accumulation of precipitation, Mirlean et al. 2000; Casartelli et al. 2008). These palustrine areas are formed by saturated sediments with significant accumulation of organic matter from decomposed plants and small animals, commonly called peat or *gyttja*. This more organic material is very important, since it is highly reactive to metals and surfaces playing an important role in driving the mobility and bioavailability of As (Recio-Vazquez et al. 2011). According to Polizzotto et al. (2008), the metalloid release may continue until either As is depleted from solids or its reduction becomes limited due to the labile organic carbon exhaustion.

Environments with ridge-dominated formations suggest As accumulation in groundwater and via atmospheric deposition (Mirlean et al. 2014), similar to As problematic areas in Asiatic deltas (Bhattacharya et al. 2002, 2009; Hoque et al. 2012). This idea is reinforced by the exclusion of other As sources, since the study area is free of volcanic deposits, as well as of alluvial and lithological contribution containing this metalloid. Based on the exposed and according to similarities of geomorphological and geological features among areas with high As concentrations, hypotheses about the significant presence of this element in groundwater of the southern Brazilian coastal plain are highlighted.

A possible As contamination in groundwaters is worthy of attention considering the importance of these environments in health and economy. Most of these aquifers are located in man-occupied areas and in suburbs, where groundwaters from artisanal wells are used for domestic supply and irrigation. So, a research should be carried out in order to show these real possibilities of contamination.

In this paper, we presented the results of As distribution in sediments and waters of a freshwater marsh, an aquifer (a palaeo-freshwater marsh), and a modern eolic dune in the coastal plain of the southern Brazil. Our main goals were to: (1) characterize the As distribution in sediment cores; (2) quantify the concentration of As in groundwater; (3) evaluate geochemical controls of As distribution along a freshwater marsh sediment core; and (4) to provide insight into the mechanisms of As mobilization in shallow groundwater systems.

Study area

Three sampling sites were selected for this study in the Patos lagoon margins (Fig. 1a). The first site was positioned in the coastal foredunes (FD—foredune; 32°09′37.4″S 52°06′21.8″W, at sea level) in Cassino beach. The second one was placed in an interdune freshwater marsh in the coastal plain (CM—current marsh; 32°10′11.2″S 52°21′02.3″W, at 12 m a.s.l.), and the third one was also in an interdune freshwater marsh but buried under eolic sands in the same coastal plain, where its shallow groundwater aquifers have already formed (BM—buried marsh; 32°04′07.1″S 52°09′47.6″W, at 9 m a.s.l.; Fig. 1b). All studied sites were located in undisturbed areas (never occupied) to avoid any type of direct anthropogenic interference.

The coastal plain is formed of unconsolidated Cenozoic sediments corresponding to the top of the sedimentary

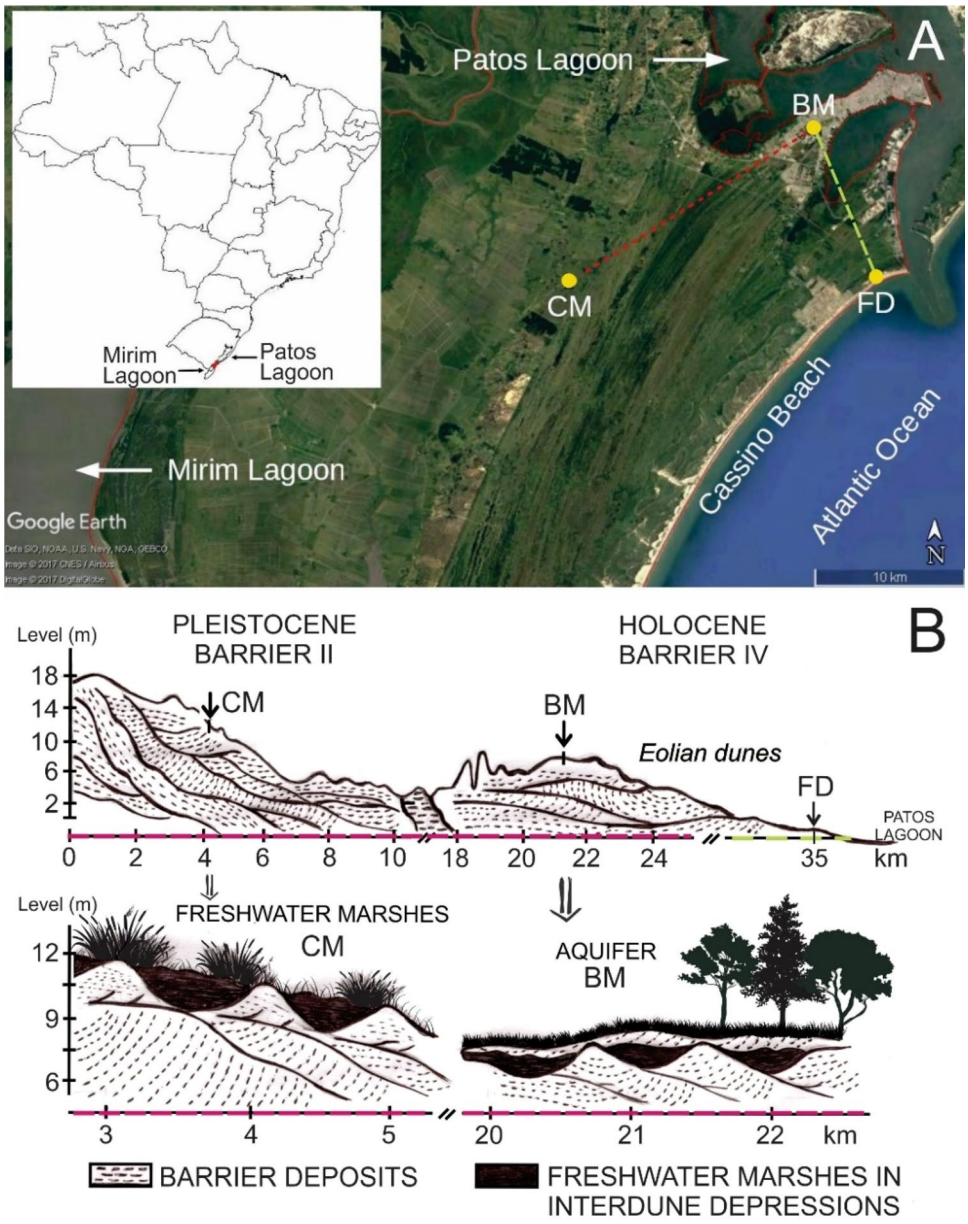

Fig. 1 **a** Location of the sampling sites in the southern Brazilian coastal plain: FD (coastal foredune), CM (current freshwater marsh in the interdune depression), and BM (aquifer in a buried freshwater marsh in the interdune depression). The red dotted line represents the distance between CM and BM (~ 18 km), and the green dotted line represents the distance between BM and FD (~ 13 km). **b** Topographic profiles of the transects (red and green dotted lines) with the location of the CM, BM, and FD and the representation of their associated environments

column of the Pelotas Basin (Barboza et al. 2008), characterized by depositional systems resulting from reworking of the surface portion due to transgressive and regressive cycles of sea level since the late Pleistocene (Buchmann et al. 2009). The FD and BM sampling sites correspond to the Holocene Barrier system (Barrier IV) with eolian deposits, formed by unconsolidated white quartz sands, and CM corresponds to the Pleistocene Barrier II system with beach and eolian facies (Fig. 1b). The sediments composing the eolic deposits mainly (> 95%) formed by fine sand (< 0.125 mm) have mineralogical composition predominantly of quartz (~ 97%), small quantity of muscovite and kaolinite, and rare grains of heavy minerals rutile e ilmenite (Tomazelli and Villwock 2005).

The eolian dunes (FD) along Cassino beach are represented by a well-developed field which varies from 2 to 8 km of width and extends over the entire southern coast (Tomazelli and Villwock 2005). Wind is a very important climatic element to be considered in the behavior of the free dunes, since these migrate towards SW in response to the high-energy wind regime from NE, covering older lands or adjacent water bodies (Tomazelli and Villwock 2005).

The freshwater marsh (CM) has SW–NE direction with 1.0 km of maximum width and predominance of *gyttja* in the interdune depressions (Fig. 1b). It is dominated by macrophyte plants with a wealth of species of Cyperaceae family followed by Poaceae and Asteraceae.

The BM aquifer is currently covered by grassland with pine and eucalyptus trees (Fig. 1b). Its groundwater system is shallow and composed by distinct layers of sediments, where some of them indicate the presence of former "freshwater marsh lenses" covered by eolian sands from dunes.

Materials and methods

Sampling, stratigraphic description, and materials preparation

The sampling was undertaken in July–August of 2016. The sediment cores were taken by 8.0-in. high-density plastic tubes, which were manually pushed into the sediment using mallet and jaws. Immediately after transportation to the laboratory, FD and BM cores were longitudinally opened with a circular saw. After stratigraphic descriptions of these cores (FAO 2006; Schoeneberger et al. 2012), subsamples of every 2 cm were taken from central position and stored in zip-lock plastic bags. The CM core was frozen as soon as it arrived into laboratory, since its sediment presented high water content which did not allow the opening of the tube. After this, to prevent loss of material, the sediment was sectioned with a clean plastic knife, and subsamples were also taken every 2 cm and immediately stored in centrifuge tubes with lids. At the time of the subsampling, the description of the CM core was performed sample by sample based on their observations, which were annotated following the same protocol used for the FD and BM cores.

The groundwater samples from the FD and BM were collected with a Push-Point™ sampler (M.H.E. Products). Only one water sample was obtained in depth of 210 cm for FD, and a total of ten water samples was taken in depths of 64–172 cm for BM. These samples were directly stored in rigorously cleaned 500 mL polypropylene bottles, placed in thermal boxes, and immediately carried to the laboratory. Water samples were filtered through 0.22-µm membranes, acidified with concentrated HNO_3, and stored in a refrigerator in duplicates one. Water samples of the CM were directly extracted from its sediment core. For the uppermost subsamples (from 0 to 22 cm) of this sediment, the pore water was separated from the defrosted sediment by centrifugation. For the undermost subsamples (from 22 to 45 cm), the water extracts were received after shaking sediment and deaerated Milli-Q water (1:1), and finally separated by centrifugation at 6000 rpm.

For the analytical determinations of the sediments, the FD, BM, and CM subsamples (material resulting from the extraction of water) were dried at about 25 °C and sieved at 2 mm.

Analytical determinations

The pH and conductivity of the water samples of all cores were determined using an advanced ISE/pH/mV/ORP/temperature meter with HI 4115 silver/sulfide combination electrode HANNA®.

The organic carbon (Corg) in the sediments was estimated based on the method for determining the organic matter (OM) by ignition in a muffle oven (Lynn et al. 1974; Goldin 1987; EMBRAPA 2018). The OM content was determined by the loss of mass of the incinerated sediment, considering the burning ranging from 105 °C/24 h to 600 °C/6 h [MO = (105 °C dry weight − 600 °C dry weight)/(105 °C dry weight × 100)]. The Corg contents were calculated by dividing the OM values by the "van Bemmelen" factor (1.724).

As, Fe, and Mn in the sediments (~2.0 g dry weight) were extracted with 5 mL Analar grade 14 M HNO_3 (Madejón and Lepp 2007). In the solid and liquid samples, As was determined by electrothermal atomic absorption spectrometry using a Perkin-Elmer 800 instrument equipped with a Zeeman background corrector and pyrolytically coated tubes with a platform. For a higher ashing temperature, $Pd(NO_3)_2$ and $Mg(NO_3)_2$ matrix modifiers were used. In solid samples, Fe and Mn contents were determined using flame (acetylene–air) atomic absorption spectrometry (AAS GBC 900 instrument).

The detection limits were calculated according to IUPAC recommendations (IUPAC 1994). Each sediment sample was analyzed in triplicate. The precision as the relative standard deviation (%RSD) was less than 4.0%, 3.5% and 5.1% for As, Fe, and Mn, respectively.

Reference material (PACS-2, National Research Council of Canada) was analyzed together with the studied samples for the accuracy control purposes. The total As, Fe, and Al concentrations of PACS-2 were 25.9 ± 1.4 mg kg^{-1}, $4.25 \pm 0.1\%$, and 453 ± 12 mg kg^{-1}, respectively, i.e. yielding As, Fe, and Mn recovery within 95% confidence limits (certificate value 26.2 ± 1.5 mg kg^{-1} for As, $4.09 \pm 0.06\%$ for Fe, and 440 ± 19 mg kg^{-1} for Mn).

The ions Na, NH_4^+, K, Ca, Mg, F^-, Cl^-, NO^{3-}, and SO_4^{2-} of the water samples were also determined. An Ion Chromatography Metrohm® apparatus was used for this. For FD core, the only sample collected (120 cm) was analyzed, while six (between 1 and 41 cm) and seven samples (between 78 and 157 cm) were, respectively, selected for BM and CM cores. The detection (LD) and quantification (QD) limits were also calculated according to IUPAC (1994) (Table S1 in supplementary material).

Statistical analysis

Principal component analysis (PCA) was performed on the geochemical data of the sediment and water samples of the

CM and BM cores in order to enable an intuitive interpretation of environmental dynamics and their interactions. The Kaiser–Meyer–Olkin (KMO) Measure of Sampling Adequacy (Kaiser 1974) and Bartlett's test of sphericity (Bartlett 1937) were used to indicate the suitability of the geochemical data for the PCA. Each principal component may provide a meaning about the geochemical processes associated. For PCA, the samples with all analytical data such as pH, conductivity, As sediment, As water, Fe, Mn, and organic carbon were used. The cations Na, NH_4^+, K, Ca, Mg, and the anions F^-, Cl^-, NO^{3-}, and SO_4^{2-} in water were not included in the analysis. This was decided after results from PCA including water principal ions had demonstrated insignificant contribution of these cations to As accumulation in sediment and its release to water (see the supplementary material; Fig. S3 and Table S3).

Except for pH, the geochemical data were log-transformed (natural logarithm) and standardized (z-scores) before PCA, as suggested for compositional data (i.e. close data sets) (Reimann et al. 2008). The PCA was performed in the correlation mode, and a varimax rotation was applied to maximize the loadings of the variables in the components (Eriksson et al. 1999). The Pearson correlation coefficients were also determined among the geochemical data in order to quantify their relations. Both principal components and correlations were analyzed in the SPSS 20.0 software.

Results and discussion

Contents of As in rocks, sediments, and soils have varied greatly depending on their mineralogical compositions and environments of formation. The rocks of the continental crust contain an average of 1.7 mg kg^{-1} (Wedepohl 1995). Sandstones are usually the poorest in As with an average of about 0.5 mg kg^{-1} (Siewers 1994). In soils, the As content varies over a wide range of concentrations from 1 to 105 mg kg^{-1}, averaging 5 mg kg^{-1} worldwide, while this interval ranges from 0.9 to 22 mg kg^{-1} in alluvial and lacustrine sediments (Reimann et al. 2009). Thus, the As content of 0.6 ± 0.5 mg kg^{-1} in the sand of the FD core (Fig. 2) almost corresponded to the average content of this metalloid in sandstones. The distribution of the As concentration did not fluctuate significantly along the FD profile

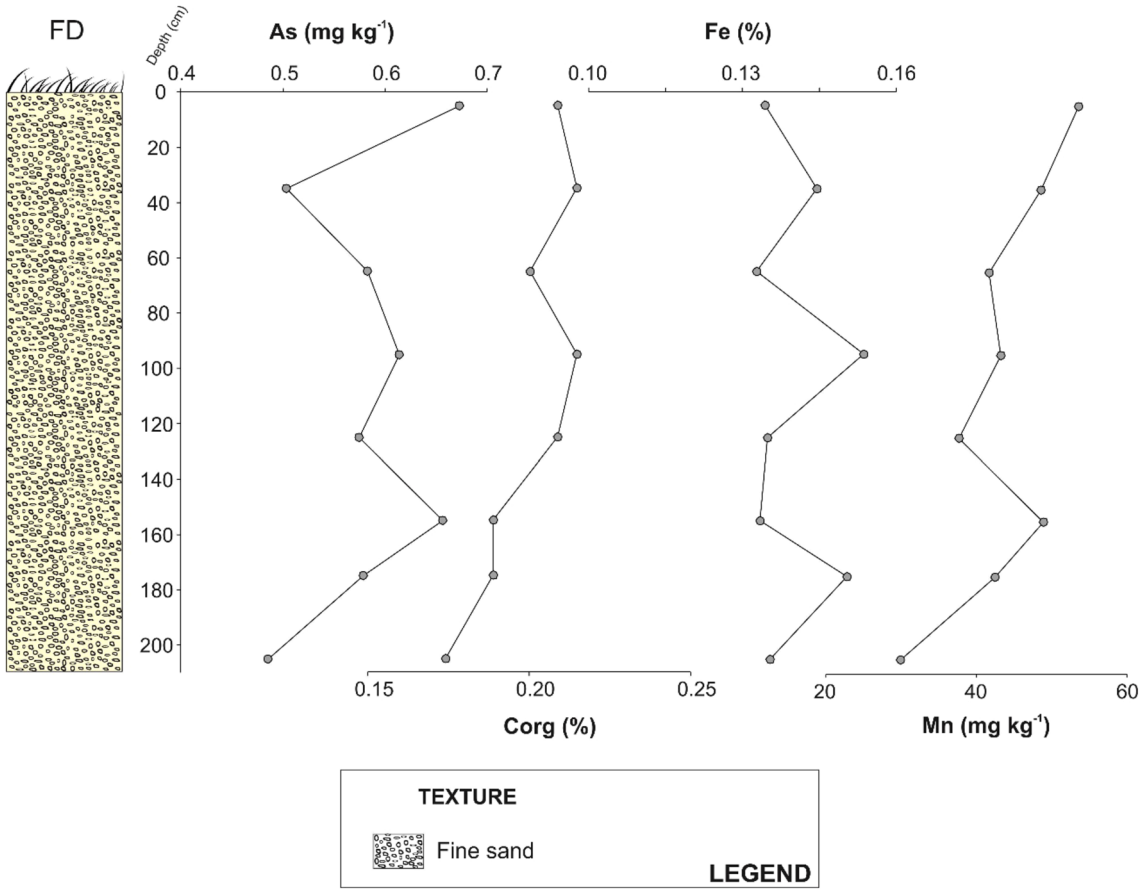

Fig. 2 Distribution of the As, Mn, Corg, and Fe contents along the FD core

down to the level of groundwater (Fig. 2), exceeding the error of analytical method, i.e., the eolian redistribution of sands did not lead to the appearance of horizons or layers markedly enriched in arsenic. Thus, the layers relatively enriched in CM and BM cores, as shown below (Figs. 3, 4), could not be the result of mechanical separation of sand deposits on dunes. The Corg (average $0.2 \pm 0.01\%$), Fe (average $0.14 \pm 0.01\%$), and Mn (average 40 ± 10 mg kg^{-1}) concentration also did not fluctuate significantly along the FD profile (Fig. 2). However, they have be highlighted by representing the background values of the sandy sediments, taking part in the formation of the interdune marshes in this

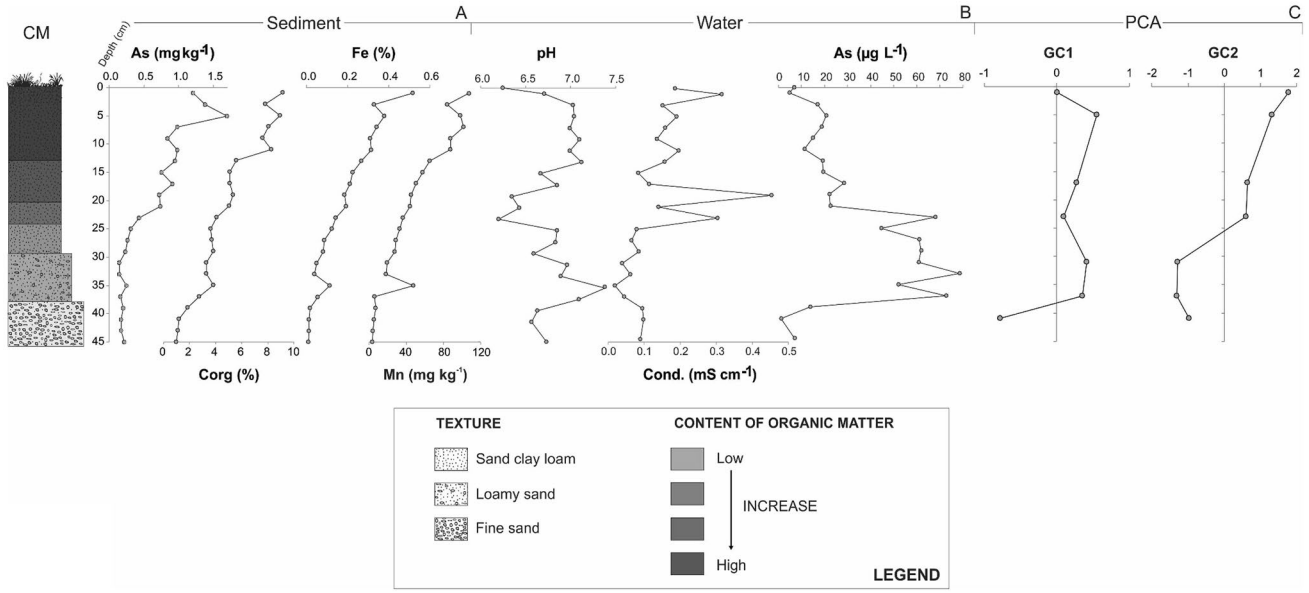

Fig. 3 **a** Distribution of the As, Mn, Corg, and Fe contents along the CM core. **b** Distribution of pH, electrical conductivity, and As concentration in the interstitial water along the CM core. **c** Record of factor scores for the two principal components extracted by PCA from the geochemical composition of the sediment and water samples of the CM core

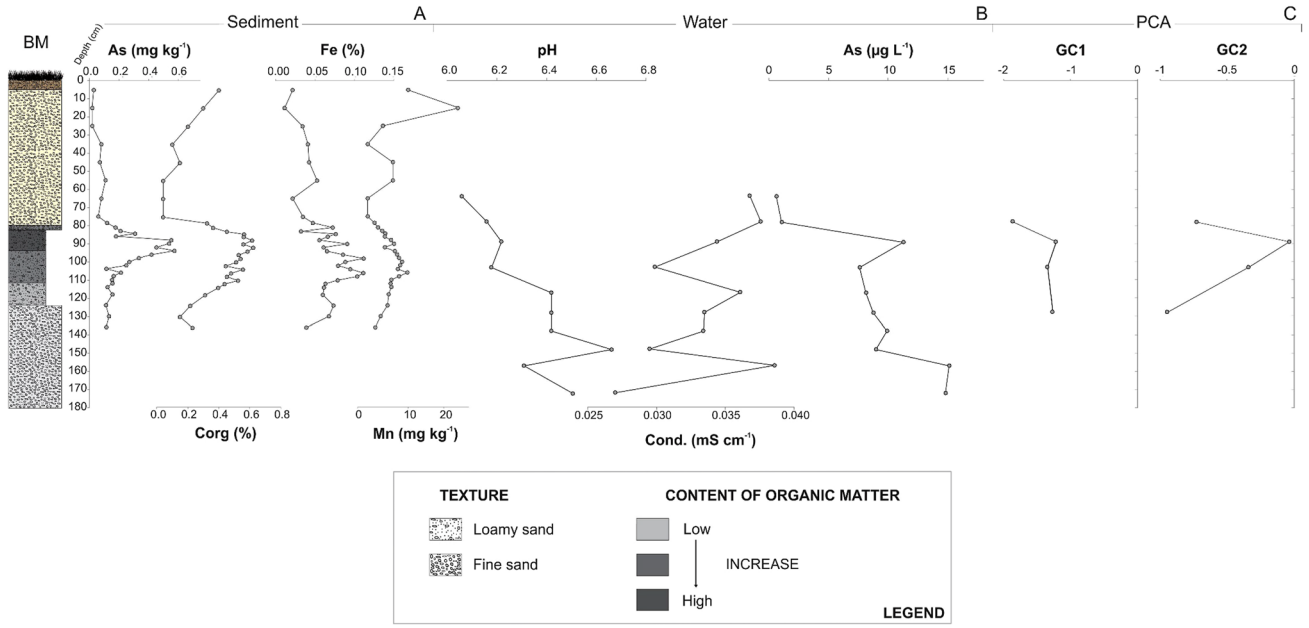

Fig. 4 **a** Distribution of the As, Mn, Corg, and Fe contents along the BM core. **b** Distribution of pH, electrical conductivity, and As concentration in groundwater along the BM core. **c** Record of factor scores for the two principal components extracted by PCA from the geochemical composition of the sediment and water samples of the BM core

study region. The groundwater in the FD (210 cm) presented 1.28 µg L^{-1} of As concentration which has been considered as a background for unaffected regions (Edmunds et al. 1989; Welch et al. 2000), in a neutral environment (pH ~ 7.3 and Cond. ~ 0.33 mS cm^{-1}). All these data demonstrate that the geochemical situation in the sandy dune deposits was not favorable for As redistribution and mobilization into groundwaters.

The distribution of the elements As, Fe, Mn, and Corg in the solid phase of the CM core demonstrated a strong general tendency of decrease from the surface to the base (Fig. 3a). The highest contents of Corg (maximum of 9.2% in 0–2 cm) in CM were found in the first 20 cm (average 7.0 ± 1.2%), while the lowest values were in the undermost layer (20–45 cm, average of 2.8 ± 1.2%) in agreement with the increase of sandy sediments reaching 0.98% at 45 cm (Fig. 3). The enrichment of Fe and Mn with values up to 0.52% and 100 mg kg^{-1} concomitantly occurred in the part with the highest concentrations of Corg in 0–2 cm interval (Fig. 3a), correspondingly.

The As distribution of the CM sediment demonstrated an almost eightfold increase of concentration in the upper 0–5 cm horizon (1.7 mg kg^{-1} dw) if compared to the same in the mineral substrate (Fig. 3a). The highest As values in the 0–20 cm interval (average 1.0 ± 0.3 mg kg^{-1} dw) coincided with the same interval with the highest OM content (Fig. 3a). In the sandy layers (20–45 cm), the values of As decreased reaching the lowest values with an average content of 0.23 ± 0.1 mg kg^{-1} dw. Similar patterns of As distribution were also observed in other sediments of interdune environments, as those in the Paraiba do Sul delta with very high concentrations (~ 270 mg kg^{-1} dw) in the *gyttja* sediments and low values (< 1.0 mg kg^{-1} dw) in the underlying sandy sediments (Mirlean et al. 2014).

Studying the distribution of As in profiles of ombrotrophic peat bogs in Scotland, Cloy et al. (2009) found that this metalloid is firmly restrained by the peat material (up to 9.7 mg kg^{-1}) at depths of 10–20 cm from the peat surface. In the same country, Küttner et al. (2014) studied the distribution of arsenic in a 3300-year-old profile of a peat bog and also found a peak concentration of As at a depth of about 15 cm concluding that As was mainly related to atmospheric pollution. In Italy, the As concentrations in sphagnum peat profiles were higher in the uppermost layers (0–20 cm) and decreased at greater depths to below the detection limit of the analytical equipment (Ukonmaanaho et al. 2004). These authors explained the As distribution by its anthropogenic deposition during past decades.

However, in many cases, the As distribution and its accumulation in the upper parts of sediments could not be attributed only to the anthropogenic effects. The common opinion is that arsenic diagenesis is strongly coupled to Fe cycling and redox conditions that are determined by organic matter remineralization in marine sediments (Widerlund and Ingri 1995; Sullivan and Aller 1996; Chaillou et al. 2003; Bone et al. 2006). According to our results, the trend of As decreasing with depth reflected the reduction and removal of this metalloid from a reactive carrier phase (e.g., metal oxide) into solution. This interpretation was supported by the As leachable that varied concurrently with Fe(II), and its diffusion upwards of the Fe-redox boundary (Widerlund and Ingri1995). A major part of As was trapped in the oxidized surface layer that forms a sediment slice (0–2 cm) relatively rich in this metalloid (Chaillou et al. 2003). A similar process of reductive dissolution of Fe(III) increased arsenic mobility and its diffusion into upper horizons was also characteristic of freshwater lakes (Deng et al. 2014). The CM core is more like sediment (and not peat or organic-rich sediments, according to Andrejko et al. 1983), and we could expect that As distribution in its profile was determined by geochemical processes developing in the sediments of open water systems.

The average content of As in the sediments of the CM core (Fig. 3a) was almost the same as its average content in the profile of the dune eolian deposits FD (Fig. 2), with 0.58 ± 0.06 and 0.60 ± 0.45 mg kg^{-1}, respectively. In view of the lack of anthropogenic sources of As in our study area, we could consider the primacy of natural geochemical processes in its redistribution in the profile of CM, whose sand sediment was completely represented by dune material. So, probably, the existence of a reducing environment during the formation of CM promoted the dissolution of Fe(III) hydroxides present on the surface of sand particles, resulting in the mobilization of As. Likewise, it was already reported for salt marshes and continental shelf sediments, where the diffusive migration of As and its sorption by Fe(III) hydroxides occurred in the upper oxic horizon (Sullivan and Aller 1996; Caetano and Vale 2002; Leal-Acosta et al. 2010; Mirlean et al. 2012) similarly to the sediment profile of CM.

The interstitial water extracted from the CM core presented low conductivity (between 0.06 and 0.45 mS cm^{-1}) and pH ~ 6.2–7.4 (Fig. 3b). A steeply rising peak delimiting the interface more organic and mineral sediments occurred between 17 and 25 cm interval, where the highest water total dissolved salts was concentrated at 19 cm. A zone with the lowest pH values (6.2–6.9) was also found at 17–25 cm. Concentrations of As in pore waters of the CM core (1.2–78.5 µg L^{-1}) were within the limits of already published data for marshy environments. The close data were reported in Broder and Biester (2015) for an ombrotrophic peatland located within the nature protection area in northwestern Germany with concentration of As in pore water between 1.2 and 3.8 µg L^{-1}, and in Wang et al. (2012) in pore waters of saltmarsh sediments in the Yangtze River estuary (China), where the As concentration ranged from 3 to 71 µg L^{-1}. The maximum of 79 µg L^{-1} at 33 cm (Fig. 3b)

was also close to those values determined in Bangladesh, the country with severe health problems due to high As concentration in groundwater (Dhar et al. 1997). However, the As distribution along this core differed from the same in pore waters of peat bogs, where peaks of As occurred in the near-surface horizons. In the CM, the maximum concentrations of soluble arsenic were found in the intermediate depths (23–37 cm) of the sediment profile (Fig. 3b), where the sediment had the highest contribution of sand followed by a constant reduction of Corg. The decrease in As concentration in the deepest part of the profile (below 37 cm) could be explained by the low content of this metalloid in the solid phase as source for pore water, as well as by a significant decrease in the OM content directly or indirectly involved in arsenic mobilization.

According the results of the KMO (0.681) and Bartlett tests (approximately Chi squared: 67.18; degree of freedom: 21; and significance level < 0.05), the geochemical data were suitable for the structure detection and the PCA was useful for interpretation of the dynamics and interactions. One first PCA was carried out containing all the geochemical data determined in sediments and water, resulting in five principal components (see in Supplementary Material; Fig. S3 and Table S3). However, the anions F^-, SO_4^{2-}, NO_3^-, Cl^- and cations Mg, NH_4, Na, Ca, K determined in water were observed in components where As in sediment or in water were not present (GC1, GC2, and GC3; Fig. S3 and Table S3). In other words, they were very little related to the As and did not help to explain the process of As sediment releasing in water (for more details, see the discussion in Supplementary Material). In this sense, another PCA was carried out without these ions, which is the one that is presented here in the manuscript.

So, two first principal components were obtained and explained about 67% of the total variance of the geochemical composition of the sediment and water (Fig. 5, Table 1). This analysis confirmed the geochemical redistribution of these elements in the diagenetic transformation processes of the CM sediment and also summarized the ideas regarding the process of As immobilization from the solid phase to the water phase supporting all that was inferred here. The first component (GC1; explained 40.51% of the geochemical data variance) showed high positive loadings (> 0.7) for pH, Mn, organic carbon (Corg), and As in water (As_w), and moderate positive loading (0.5–0.7) for conductivity (Cond) (Table 1). This component considers that part of the organic matter (60% of Corg proportion variance; Fig. 5) supported the presence of As in water, which was corroborated by the correlation coefficient between them ($r = 0.55$; Table 2). Corg, a redox reactive compound, mediates the redox transformation of As solid-phase and its release to water, therefore presenting a critical role in controlling As mobility. The Mn element may form Mn–organic matter complex ($r = 0.63$ between Mn and Corg), mainly favored by the alkaline pH range ($r = 0.59$ between pH and Mn). Although GC1 was not the main factor controlling the contents of the arsenic in sediment (As_s), there was a significant proportion of its variance associated with this component (14%; Fig. 5). As_s was correlated with Corg ($r = 0.63$) and Mn ($r = 0.65$), and this may indicate that a part of As_s was supported by the Mn-organic matter complex to a lesser extent.

The second component (GC2; explained 26.83% of the geochemical data variance) presented high positive loadings for Fe and As_s (Table 1). This component indicated

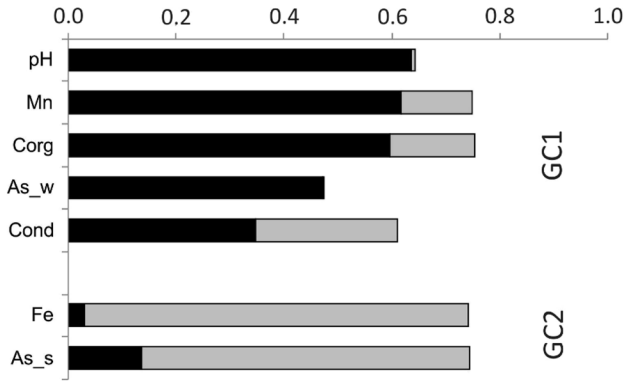

Fig. 5 Fractionation of communalities of the geochemical variables used in the PCA of the sediment and water samples for the CM and BM cores. The communality of each variable (proportion of variance explained by each component) corresponds to the total length of the bar. The sections of each bar represent the proportion of variance in each component. The variables are ordered by the component with the largest share of variance. *Corg* organic carbon, *Cond* conductivity, *As_s* arsenic in sediment, *As_w* arsenic in water

Table 1 Factor loadings for the two components extracted by PCA of the geochemical composition of the sediment and water samples of the CM and BM cores

	GC1	GC2
pH	**0.80**	
Mn	**0.79**	0.37
Corg	**0.77**	0.40
As_w	**0.69**	
Cond	**0.59**	0.51
Fe	−0.18	**0.84**
As_s	0.37	**0.78**
Eigenv	3.41	1.30
Var (%)	40.51	26.83

Corg organic carbon, *Cond* conductivity, *As_s* arsenic in sediment, *As_w* arsenic in water, *Eigenv* eigenvalues, *Var (%)* percentage of explained variance, *GC1* first principal component, *GC2* second principal component, The highest factor loading for each geochemical attribute is in bold

Table 2 Correlation matrix of the geochemical composition of the sediment and water samples of the CM and BM cores

	As_s	Corg	Fe	Mn	pH	Cond	As_w
As_s	1.00	0.63[a]	0.63[a]	0.65[a]	0.2	0.53[a]	0.11
Corg		1.00	0.47[b]	0.63[a]	0.45[b]	0.63[a]	0.55[a]
Fe			1.00	0.30	0.08	0.48[b]	0.10
Mn				1.00	0.59[a]	0.54[a]	0.26
pH					1.00	0.52[a]	0.34
Cond						1.00	0.21
As_w							1.00

$N = 24$

[a]Correlation is significant at the 0.01 level (2-tailed)

[b]Correlation is significant at the 0.05 level (2-tailed)

that most of proportion variance of Fe (71% of proportion variance; Fig. 5) supported the adsorption of As_s (61% of proportion variance; Fig. 5). These elements had a high correlation ($r = 0.63$; Table 2), suggesting that the Fe element was most likely in Fe-bearing minerals form, such as Fe(III) hydroxides (goethite and hydrogoethite, for example), and the As(V) was strongly adsorbed on them.

The distributions of scores for the GC1 in CM (Fig. 3c) showed that these were positive and remained high even in the sand layers (Fig. 3c). So, the organic matter from the layers with the highest OM content triggered the process of As release to water. The As in soluble state (mobile) could be redistributed in depth by vertical downward infiltration, making the underlying layers even more enriched in this element. The changes in the GC2 scores (Fig. 3c) showed a good agreement with the stratigraphic descriptions, and the decrease of the scores toward the base was evident. The highest values of GC2 were in the more organic layers where also occurred the highest Fe and As concentrations in the sediments, and the lowest scores in the sandy underlying layers poorer in this elements.

In the BM core (aquifer), the distribution of the geochemical elements along this profile was different (Fig. 4a), where a strong separation of two data sets at 75 cm was remarkable showing differentiated distribution patterns between 0 and 75 cm and 75–137 cm intervals. As general trends, As and Fe showed increasing behavior in the upper sediment (0–75 cm) interval, while Corg and Mn presented opposite trend. In the bottom of the sediment (below 75 cm), all elements (As, Corg, Fe, and Mn) showed increasing behaviors (for As and Corg up to ~ 93 cm and for Fe and Mn up to 106 cm) and a general abrupt decreasing toward the base after that. This distribution, especially below 88 cm, was similar to that in the CM core (Fig. 3a). In the whole core, As concentrations varied from 0.1 to 0.6 mg kg^{-1} (average 0.2 ± 0.1 mg kg^{-1}), Corg between 0.2 and 0.6% (average 0.5 ± 0.1%), Fe between 0.03 and 0.11% (average 0.07 ± 0.02%), and Mn between 3 and 10 mg kg^{-1} (average 7 ± 2 mg kg^{-1}).

The layers with the highest contents of Corg in the BM core (Fig. 4a) were the same ones with the highest values of OM (first two loamy sand layers, 83–114 cm interval), while the most impoverished were those with the highest contents of sand sediment (the first 0–79 cm and 114–136 cm intervals; Fig. 4a). The layers with more organic contents were positioned sandwiched between sand packs, showing very abrupt changes of Corg concentrations with well-marked upper and lower limits. This discontinuity supported the idea about the formation of an ancient marsh between old dunes in an inner part of the beach ridge complex (Figs. 1b, 6), since the most basal part of the core presented quartz sand. After a time, this ancient marsh was buried by sandy sediments as a sequence of dune dynamics (Figs. 1b, 6).

The Mn has normally tended to move to the surface layers farther than Fe by the geochemical process of redistribution, as observed in the BM core (Fig. 4a). Below 75 cm, Fe concentration continued increasing and Mn remained the same. The highest concentrations of these elements were found between 84 and 106 cm interval, corresponding to the first two sand organic layers, where the maximum value for Fe (0.11%) occurred in 98 cm and 106 cm and for Mn (10 mg kg^{-1}) in 106 cm (Fig. 4a). In the second part of this core, Fe distribution resembled a see-saw model with sharp variations in depth. Probably, the water table fluctuations constantly interfered in the Fe oxy-reduction processes when there was a marsh. An abrupt decrease in concentration of both elements' concentrations to very low values occurred in the most basal part of this profile (106–136 cm) followed by an accentuated increase in sand content. This behavior was similar to the tendency already observed in the lower part of the CM sediment core (Fig. 3a).

Similar to the Corg, the highest concentrations of As also occurred in the "sandwiched" layers with values reaching 0.6 mg kg^{-1} dw at 94 cm depth (Fig. 4a). In the sandy uppermost and undermost layers of the core, the lowest concentrations (average 0.2 ± 0.1 mg kg^{-1} dw) were observed. Similarly, higher As concentrations (30.2 mg kg^{-1} dw) were also seen in more organic layers of buried sediments in the

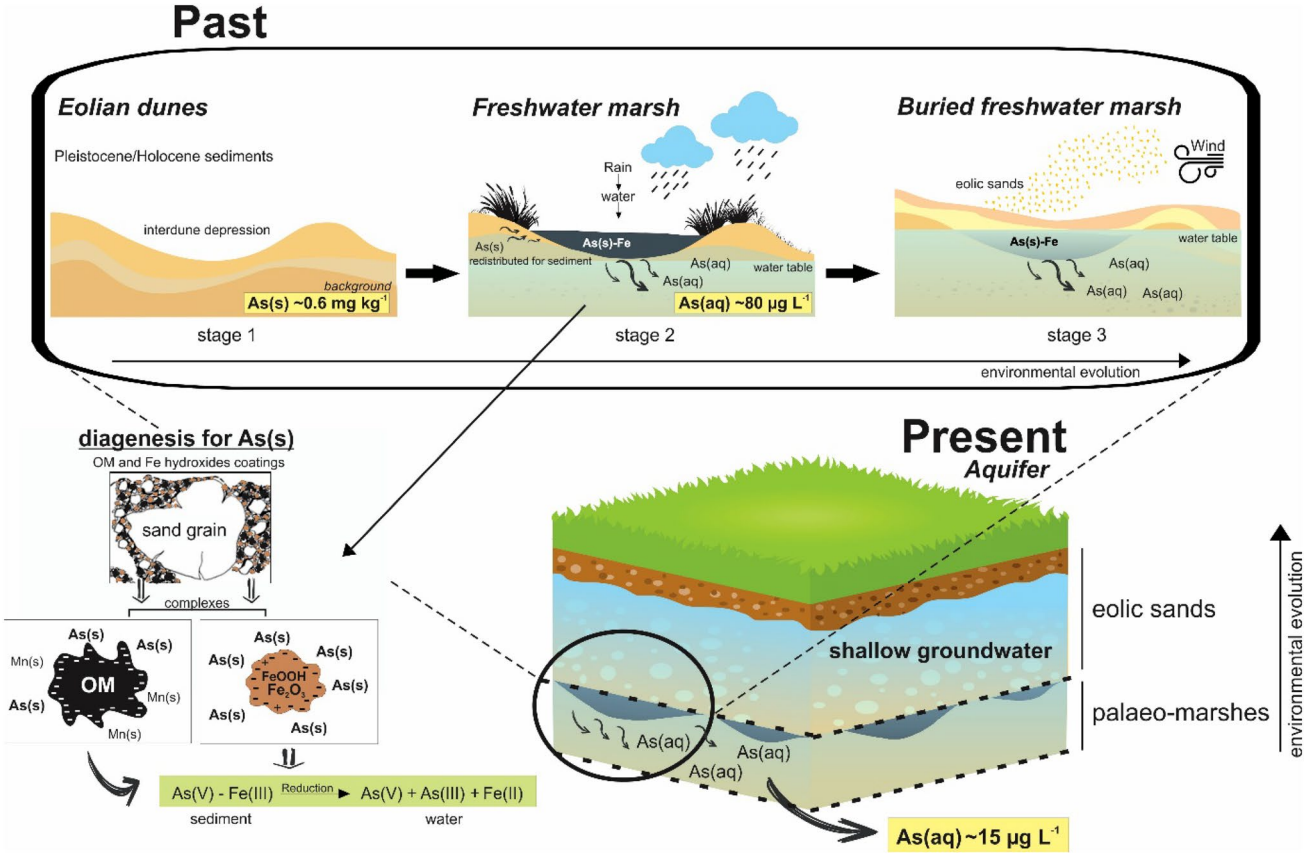

Fig. 6 Representation of the arsenic geochemistry processes in the different environments in the southern Brazilian coastal plain

Paraiba do Sul delta, while the lowest values (~ 0.8 mg kg^{-1} dw) were observed in sand-intensive sediments (Mirlean et al. 2014). The As mean concentrations were close to those maximums verified in the FD core. Probably, the As from sandy sediments associated with buried freshwater marshes was partly remobilized and removed by lateral groundwater flow from the BM.

The groundwater of the BM aquifer also demonstrated low conductivity, but even lower (0.027–0.039 mS cm^{-1}), and was slightly more acidic (pH values between 6.1 and 6.7; Fig. 4b) than that determined in the CM core. Even with little variation, the conductivity and pH distributions throughout of the BM core were similar to the second half of the CM core (below 17 cm; Fig. 3b). In the most basal part of BM core (Fig. 4b), both parameters presented a reverse pattern where the conductivity generally decreased while pH increased. In the upper sand layers of this core (up to 78 cm), water-extractible As concentrations were significantly lower (average 0.87 ± 0.31 µg L^{-1}) than in the loamy sand and sand layers (average 10.6 ± 2.93 µg L^{-1}) of the lowest part (78–172 cm) of the profile (Fig. 4b). Two main peaks of As were verified at 89 cm (11.25 µg L^{-1}) and at 157 cm (15.11 µg L^{-1}).

The distributions of GC1 scores in BM (Fig. 4c) obtained by PCA showed an increase in the layers with higher OM content, and remained more or less constant in agreement with increase of sand sediment toward the base, agreeing with As increasing concentrations in depth. The GC2 scores (Fig. 4c) showed a slight increase in the layers with higher content in OM and an abrupt decrease after this, i.e., the highest As values occurred within the layers more enriched in Fe.

The reduction of As in the BM sediments (Fig. 4a), that form the modern shallow groundwater table, as a whole resembled that one in the CM core (Fig. 3a). In the intermediate part of the BM core, which was more enriched with OM, an almost fivefold increase of As concentration was observed. However, this sediment was generally depleted in As (about two times) if compared to the CM core. A significant decrease in As content in buried marsh sediments after their transformation into a shallow aquifer could be explained by a lateral outflow of soluble compounds into the local drainage system (Fig. 6). A similar decrease in the arsenic concentration was assumed in the rocks of the aquifers of Southeast Asia (Polizzotto et al. 2008). The authors supposed that the rates of As release would initially be high,

due to the large pool of available solid-phase arsenic, and this release would continue until the As was pretty much depleted from sediments to groundwater.

The down-core As distribution in the water of BM showed a multiple increase in its concentration (more than 20 times) in the part of the core represented by the CM sediments. The sanitary limit of arsenic (10 μg L^{-1}) for drinking water was exceeded in three BM water samples. Concentrations above this threshold have been common in aquifers of the arsenic-contaminated areas (Bhattacharya et al. 1997; Bundschuh et al. 2012; Yang et al. 2014). However, groundwaters with high-As content have not been necessarily related to areas with high concentrations from source rocks (Smedley and Kinniburgh 2002). For example, As-affected groundwaters in the Bengal Basin are associated with sediments having total As concentrations in the range between 2 and 20 mg kg^{-1}, i.e., not exceptional by the world-average values (Dhar et al. 1997). In the BM, the As content in the source sediments was extremely low, barely reaching the average value of 0.25 mg kg^{-1}. However, even this very low content was able to provide relatively high As concentration in the groundwater under the reducing conditions of the organically rich CM sediments.

Regarding geochemistry, the described enrichment of the BM groundwater was similar to the processes known for the aquifers of alluvial plains and deltas composed of sandy sediments with interlayers enriched in OM (Polizzotto et al. 2008; Datta et al. 2014). Although relatively low, but still exceeding the limit for drinking water, the As concentration in the BM groundwater could be expected by higher contents in the neighborhood under the similar hydrogeological conditions. The As concentration in the groundwater of the Paraiba do Sul delta presented different values ranging from low 2 μg L^{-1} to very high 600 μg L^{-1} in wells of the same depth located at a small distance (some hundred meters) from each other (Mirlean et al. 2012). According this previous study, the "spotting" of anomalies within a single aquifer was explained by the mosaic distribution of the lenses of the marsh and lagoon sediments under the overlapping eolian sands. In the case of the Southern Brazilian coastal plain, we could expect the same mosaic distribution of As in groundwater. Figure 6 represents in the whole the geochemistry of the process cited here related to arsenic dynamics in the different environments in the southern Brazilian coastal plain, encompassing modern eolic dune, freshwater marsh, and aquifer. The lack of data about As occurrence in groundwaters in the Brazilian coastal plains has been explained by the strong prevalence of surface sources in drinking water supply. Groundwater for drinking purposes is only used by the population in remote areas deprived of centralized water supply, and the quality control of waters in artesian wells is very limited. However, similar problems to those in some Asian countries are not excluded in the future for Brazil, if the pollution of surface water courses will force the population to intensively use groundwater for drinking supply as an alternative.

Conclusion

Barrier sand dunes of the study area consist mainly of fine quartz sand contain low quantity of arsenic (0.6 mg kg^{-1}). Groundwater under these dunes also contains a background amount of arsenic slightly exceeding 1 μg L^{-1}. In the sediments of modern interdune marshes under suboxic conditions, As is mobilized from the eolic sands and its redistribution occurs along sediment profile. The maximum arsenic concentration occurs at the marsh surface (0–5 cm) and is synchronous with the Fe peak. The migration of As in marsh ambient undergoes well-described desorption from solids upon Fe(III) and As(V) reduction. This process involves a strong As enrichment (up to 79 μg L^{-1}) of pore waters in the marsh sediments. After the overlapping of interdune marshes with eolic sands, high As content is maintained overcoming the sanitary limit of 10 μg L^{-1} for drinking water in groundwater.

Southern Brazilian coastal plain is probably an arsenic-contaminated area for groundwater, which can be confirmed in future by more extensive hydrogeochemical studies in this region.

Acknowledgements The research was funded by Coordination for the Improvement of Higher Education Personnel (grant to I.H.T—post doctoral scholarship PNPD/CAPES) and National Council for Scientific and Technological Development (CNPq)/Brazil (grant to A.F—graduation scholarship PIBIC/CNPq 137792/2016-6). We are grateful to Carlos Francisco Ferreira de Andrade (Federal University of Rio Grande) for lending of the *pushpoint sampler*.

Compliance with ethical standards

Conflict of interest All the authors declare no conflict of interests regarding this manuscript.

References

Alexakis D (2011) Diagnosis of stream sediment quality and assessment of toxic element contamination sources in East Attica, Greece. Environ Earth Sci 63:1369–1383

Alexakis D, Gamvroula D (2014) Arsenic, chromium, and other potentially toxic elements in the rocks and sediments of Oropos-Kalamos basin, Attica. Greece. Appl Environ Soil Sci 2014:718534. https://doi.org/10.1155/2014/718534

Andrejko MJ, Fiene F, Cohen AD (1983) Comparison of ashing techniques for determination of the inorganic content of peats. In: Jarret PM (ed) Testing of peats and organic soils. American Society for Testing and Materials, Philadelphia, pp 5–20

Barboza EG, Rosa MLCC, Ayup-Zouain RN (2008) Cronoestratigrafia da Bacia de Pelotas: uma revisão das sequências deposicionais. Gravel 6(1):125–138

Bartlett MS (1937) Properties of sufficiency and statistical tests. Proc R Soc A Math Phys 160:268–282

Bhattacharya P, Chatterjee D, Jacks G (1997) Occurrence of arsenic-contaminated groundwater in alluvial aquifers from delta plains, eastern India: options for safe drinking water supply. Int J Water Resour D 13:79–92

Bhattacharya P, Jacks G, Ahmed KM, Routh J, Khan AA (2002) Arsenic in groundwater of the Bengal delta plain aquifers in Bangladesh. Bull Environ Contam Toxicol 69:538–545

Bhattacharya P, Hasan MA, Sracek O, Smith E, Ahmed KM, von Brömssen M, Huq SM, Naidu R (2009) Groundwater chemistry and arsenic mobilization in the Holocene flood plains in south-central Bangladesh. Environ Geochem Health 31:23–43

Bone SE, Gonneea ME, Charette MA (2006) Geochemical cycling of arsenic in a coastal aquifer. Environ Sci Technol 40:3273–3278

Borba RP, Figueiredo BR, Matschullat J (2003) Geochemical distribution of arsenic in waters, sediments and weathered gold mineralized rocks from Iron Quadrangle, Brazil. Environ Geol 4:39–52

Broder T, Biester H (2015) Hydrologic controls on DOC, As and Pb export from a polluted peatland—the importance of heavy rain events, antecedent moisture conditions and hydrological connectivity. Biogeosciences 12:4651–4664

Buchmann FSC, Caron F, Lopes RP, Ugri A, de Lima LG (2009) Panorama geológico da Planície Costeira do Rio Grande do Sul. In: Ribeiro AM, Bauermann SG, Scherer CS (eds) Quaternário do Rio Grande do Sul. Grafica Palloti, Porto Alegre, pp 35–56

Bundschuh J, Litter MI, Parvez F, Román-Ross G, Nicolli HB, Jean J-S, Liu C-H, López D, Armienta MA, Guilherme LRG, Cuevas AG, Cornejo L, Cumbal L, Toujaguez R (2012) One century of arsenic exposure in Latin America: a review of history and occurrence from 14 countries. Sci Total Environ 429:2–35

Caetano M, Vale V (2002) Retention of arsenic and phosphorus in iron-rich concretions of Tagus salt marshes. Mar Chem 79:261–271

Casartelli MR, Mirlean N, Peralba MC, Barrionuevo S, Gómez-Rey MX, Madeira M (2008) An assessment of the chemical composition of precipitation and throughfall in rural-industrial gradient in wet subtropics (southern Brazil). Environ Monit Assess 144:105–116

Chaillou G, Schafer J, Pierre Anschutz P, Lavaux G, Blanc G (2003) The behaviour of arsenic in muddy sediments of The Bay of Biscay (France). Geochim Cosmochim Acta 67:2993–3003

Cloy JM, Farmer JG, Graham MC, Mackenzie AB (2009) Retention of As and Sb in ombrotrophic peat bogs: records of As, Sb, and Pb deposition at four Scottish sites. Environ Sci Technol 43:1756–1762

Das D, Chatterjee A, Mandal BK, Samanta G, Chakraborti D, Chanda B (1995) Arsenic in groundwater in six districts of West Bengal, India: the biggest arsenic calamity in the world. Part 2. Arsenic concentration in drinking water, hair, nails, urine, skin-scale and liver tissue (biopsy) of the affected people. Analyst 120:917–924

Datta S, Johannesson KH, Mladenov MS, Sankar MS, Ford S, Vega M, Neal A, Kibria MD, Krehel A, Hettiarachchi G (2014) Groundwater-sediment sorption mechanisms and role of organic matter in controlling arsenic release into aquifer sediments of Murshidabad area (Bengal basin) India. In: Litter MI, Nicolli HB, Meichtry M, Quici N, Bundschuh J, Bhattacharya P, Naidu R (eds) One century of the discovery of arsenicosis in Latin America (1914–2014). Taylor & Francis, London, pp 95–97

de Figueiredo BR, Borba RP, Angélica RS (2007) Arsenic occurence in Brazil and human exposure. Environ Geochem Health 29:109–118

Deng T, Wu Y, Yu X, Guo Y, Chen YW, Belzile N (2014) Seasonal variations of arsenic at the sediment–water interface of Poyang Lake, China. Appl Geochem 47:170–176

Dhar RK, Biswas BK, Samanta G, Mandal BK, Chakraborti D, Roy S, Jafar A, Islam A, Ara G, Kabir S, Khan AW, Ahmed SA, Hadi SA (1997) Groundwater arsenic calamity in Bangladesh. Curr Sci 73:48–59

Diwakar J, Johnston SG, Burton ED, Shrestha SD (2015) Arsenic mobilization in an alluvial aquifer of the Terai region. Nepal. J Hydrol Reg Stud 4(A):59–79

Edmunds WM, Cook JM, Kinniburgh DG, Miles DL, Trafford JM (1989) Trace-element occurrence in British groundwaters. Res. Report SD/89/3. British Geological Survey, Keyworth

Embrapa-Empresa Brasileira de Pesquisa Agropecuária (2018) Sistema Brasileiro de Classificação de Solos, 5th edn. Embrapa Solos, Rio de Janeiro

Eriksson L, Johansson E, Kettaneh-Wold N, Wold S (1999) Introduction to multi- and megavariate data analysis using projection methods (PCA & PLS). Umetrics AB, Umea

FAO-Food and Agriculture Organization (2006) Guidelines for soil description, 4th edn. Management Service, Rome

Gamvroula D, Alexakis D, Stamatis G (2013) Diagnosis of groundwater quality and assessment of contamination sources in the Megara basin (Attica, Greece). Arab J Geosci 6:2367–2381

Goldin A (1987) Reassessing the use of loss-on-ignition for estimating organic matter content in noncalcareous soils. Commun Soil Sci Plan 18:1111–1116

Guo H, Zhang B, Li Y, Berner Z, Tang X, Norra S, Stüben D (2011) Hydrogeological and biogeochemical constrains of arsenic mobiliz ation in shallow aquifers from the Hetao basin, Inner Mongolia. Environ Pollut 159:876–883

Hoque MA, McArthur JM, Sikdar PK (2012) The palaeosol model of arsenic pollution of groundwater tested along a 32 km traverse across West Bengal, India. Sci Total Environ 43:157–165

IUPAC (1994) Analytical methods committee. Analyst 119:16–32

Johannesson KH, Tang J (2009) Conservative behavior of arsenic and other oxyanion-forming trace elements in an oxic groundwater flow system. J Hydrol 378:13–28

Kaiser H (1974) An index of factor simplicity. Psychometrika 39:31–36

Kumar A, Adak P, Gurian PL, Lockwood JR (2010) Arsenic exposure in US public and domestic drinking water supplies: a comparative risk assessment. J Expo Sci Environ Epidemol 20:245–254

Küttner A, Mighall TM, De Vleeschouwer F, Mauquoy D, Martínez Cortizas A, Foster IDL, Krupp E (2014) A 3300-year atmospheric metal contamination record from Raeburn flow raised bog, south west Scotland. J Archaeol Sci 44:1–11

Leal-Acosta L, Shumilin E, Mirlean N, Sapozshnikov D, Gordeev V (2010) Arsenic and mercury contamination of sediments of geothermal springs, Mangrove Lagoon and the Santispac Bight, Bahia Concepcion, Baja California Peninsula. B Environ Contam Toxicol 85:609–613

Lin HJ, Sung TI, Chen CY, Guo HR (2013) Arsenic levels in drinking water and mortality of liver cancer in Taiwan. J Hazard Mater 262:1132–1138

Lynn WC, McKinzie WE, Grossman RB (1974) Field laboratory tests for characterization of Histosols. In: Aandahl AR, Buol SW, Hill DE, Bailey HH (eds) Histosols: their characteristics, classification and use. Soil Science Society of America Journal, Madison, pp 11–20

Madejón P, Lepp NW (2007) Arsenic in soils and plants of woodland regenerated on an arsenic contaminated substrate: a sustainable natural remediation? Sci Total Environ 379:256–262

Mirlean N, Vanz A, Baisch P (2000) Sources and levels of rain acidity in the region of the Rio Grande City, RS, Brazil. Quím Nova 23:590–593

Mirlean N, Medeanic S, Garcia FA, Travassos MP, Baisch P (2012) Arsenic enrichment in shelf and coastal sediment of the Brazilian subtropics. Cont Shelf Res 35:129–136

Mirlean A, Baisch P, Diniz D (2014) Arsenic in groundwater of the Paraiba do Sul delta, Brazil: an atmospheric source? Sci Total Environ 482–483:148–156

Morton WE, Dunette DA (1994) Health effect of environmental arsenic. In: Nriagu JO (ed) Arsenic in the environment, part II: human and ecosystem effects. Wiley, New York, pp 17–34

Nickson RT, McArthur JM, Burgess WG, Ahmed KM, Ravenscroft P, Rahman M (1998) Arsenic poisoning of Bangladesh groundwater. Nature 395:338

Nickson RT, McArthur JM, Shrestha B, Kyaw-Myint TO, Lowry D (2005) Arsenic and other drinking water quality issues, Muzaffargarh District, Pakistan. Appl Geochem 20:55–68

Polizzotto ML, Kocar BD, Benner SG, Sampson M, Fendorf S (2008) Near-surface wetland sediments as a source of arsenic release to ground water in Asia. Nature 454:505–508

Recio-Vazquez L, Garcia-Guinea J, Carral P, Alvarez AM, Garrido F (2011) Arsenic mining waste in the catchment area of the Madrid Detrital Aquifer (Spain). Water Air Soil Pollut 214:307–320

Reimann C, Filzmoser P, Garrett R, Dutter R (2008) Statistical data analysis explained: applied environmental statistics with R. Wiley, Chichester

Reimann C, Matschullat J, Birke M, Salminen R (2009) Arsenic distribution in the environment: the effects of scale. Appl Geochem 24:1147–1167

Rodríguez-Lado L, Sun G, Berg M, Zhang Q, Xue H, Zheng Q, Johnson CA (2013) Groundwater arsenic contamination throughout China. Science 341:866–867

Schoeneberger PJ, Wysocki DA, Benham EC, Staff Soil Survey (2012) Field book for describing and sampling soils, Version 3.0. Natural Resources Conservation Service, USDA, National Soil Survey Center, Lincoln

Siewers U (1994) The geochemical atlas of Finland—part 2: till. In: Koljonen T (ed) Chemical geology. Geological Survey of Finland, Espoo, pp 377–378

Smedley PL, Kinniburgh DG (2002) A review of the source, behavior and distribution of arsenic in natural waters. Appl Geochem 17:517–568

Smith A, Goycolea M, Haque R, Biggs ML (1998) Marked increase in bladder and lung cancer mortality in a region of Northern Chile due to arsenic in drinking water. Am J Epidemiol 147:660–669

Sullivan KA, Aller RC (1996) Diagenetic cycling of arsenic in Amazon shelf sediments. Geochim Cosmochim Acta 60:1465–1477

Tomazelli LJ, Villwock JA (2005) Mapeamento Geológico de Planícies Costeiras: o Exemplo da Costa do Rio Grande do Sul. Gravel 3:109–115

Ukonmaanaho L, Nieminen TM, Rausch N, Shotyk W (2004) Heavy metal and arsenic profiles in ombrogenous peat cores from four differently loaded areas in Finland. Water Air Soil Poll 158:277–294

Wang Y, Zhou L, Zheng X, Qian P, Wu Y (2012) Dynamics of arsenic in salt marsh sediments from Dongtan wetland of the Yangtze River estuary. J Environ Sci 24:2113–2121

Wedepohl KH (1995) The composition of the continental crust. Geochim Cosmochim Acta 59:1217–1232

Welch AH, Westjohn DB, Helsel DR, Wanty RB (2000) Arsenic in ground water of the United States: occurrence and geochemistry. Ground Water 38:589–604

Widerlund A, Ingri J (1995) Early diagenesis of arsenic in sediments of the Kalix River estuary, northern Sweden. Chem Geol 125:185–196

World Health Organization (2011) Guidelines for drinking-water quality, 4 edn. http://www.who.int/water_sanitation_health/publications/2011/dwq_guidelines/en. Accessed 25 Oct 2018

Yang N, Winkel LHE, Johannesson KH (2014) Predicting geogenic arsenic contamination in shallow groundwater of South Louisiana, United States. Environ Sci Technol 48:5660–5666

Publisher's Note Springer Nature remains neutral with regard to jurisdictional claims in published maps and institutional affiliations.